BODE PLOT STABILITY ASSESSMENT FOR THREE PARALLELED INVERTERS-CONNECTED TO GRID

P.Vinod Kumar*M.Rajarao, K.Vijay Kumar *****
* Department of Electrical and Electronic Engineering, DIET.
** Department of Electrical Engineering, DIET.
*** Department of Electrical Engineering, DIET.

Abstract:- In this work gives the idea of investigation on Harmonic commerce between current controllers used in multi paralleled inverters connected to grid. The harmonic instability problem is point out and solved by impedance based stability criterion under the consideration of dynamic behaviour of the grid. The causes for stabilized/destabilize the inverter by varying grid impedance and it is point out and solved by the passivity-based analysis and the impedance-based stability criterion. Beyond, case studies are given, which give the idea of the non-passive nature of multi paralleled inverters connected to grid under the consideration of dynamic behaviour of the grid by inserting connections of other grid connected inverters. After, the Time domain simulation results of multi paralleled inverters connected to grid are provided in the MATLAB-Simulink area in brood nature. The harmonic commerce problems are occurred in current power system and it can be assessed by the impedance-based stability analysis through shoot those problems.

1. INTRODUCTION

In current and future days, renewable energy sources are developed to overcome the future load demand and they are now expected future electric supplies and commercialized. Renewable sources may be solar, wind or geothermal. When these sources are interfaced with grid and we can use the voltage source or current source inverters based on their own advantages. when PV voltage source inverter are connected in parallel to the grid then there is possibility of harmonic instability problem arise, which is mainly caused by the commerce of inner current control loops with respect to LCL-filter parameters and grid impedance [1],[2] may exhibit resonance amplification in a wide frequency range as compared to fundamental frequency, this problem effects the PV inverters are suddenly shut-down occurs unexpectedly[3] and Each PV inverter is designed individually stable as per grid connection standards [2], the quality of the power at the point of common coupling (PCC) may not be good. [4]. Recent research work shows the impedance commerce between the multiple inverters may cause two problems, these are (1) Resonance amplification (2) The consequent harmonic instability. The above two problems are analysed and solved by impedance base stability criterion (IBSC) analysis (or) passivity based analysis, the impedance based stability criterion (IBSC) was used to design the input filters for DC-DC converters [5], [6], in earlier days. Nowadays the IBSC analysis is applied to multi paralleled inverters connected to grid to study the harmonic commerce problems of the current controllers used in the AC distribution power system, the system stability is analysed by nyquist plot analysis using minor loop gain and from the nyquist plot analysis the system is stable when there are no encirclements of (-1, j0) point otherwise the system unstable. The concept of passivity originated in control engineering, has recently been gaining attention [7] and it provides phase angle based design guideline for the all connected subsystems and each subsystem must have phase angle range between $[-90^{\circ},90^{\circ}]$,then the system is in stable otherwise unstable.

2. Modelling of Inverter Output Impedance

The single-phase representation of a three-phase grid connected inverter with grid-current control is illustrated in Figure 1(a). In order to model the inverter output impedance, the averaged switching model is used as illustrated in Figure 1(b). In addition to the filter in the control loop, there is a current controller (G_C), a time delay from the computation and pulse width modulation (G_D) [8], [9], and a modulator gain K_{PWM} defined as:

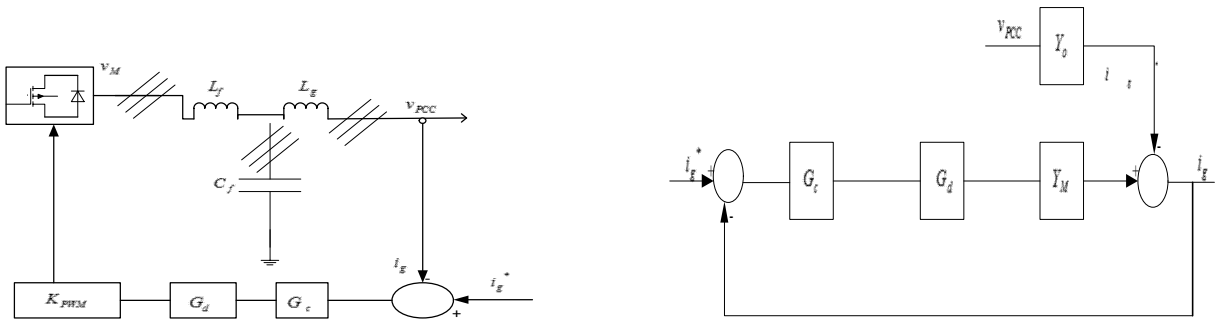

Figure1.(a) Single-phase representation of LCL-filtered inverter with grid current control, 1(b). Averaged switching model of the grid inverter.

$$G_C(s) = K \tag{1}$$

$$G_D(s) = e^{-1.5T_S S} \tag{2}$$

$$K_{PWM} = 1 \tag{3}$$

The inverter output to filter input relation is taken from Figure. 1(a) ignoring the parasitic resistances of the passive components can be defined as:

$$Y_O(S) = \frac{-i_g}{v_{PCC}}|_{v_M=0} = \frac{s^2C_fL_f + 1}{s(s^2C_fL_fL_g + L_f + L_g)} \tag{4}$$

The filter output to grid (or) load relation is given by

$$Y_M(S) = \frac{i_g}{v_M}|_{v_{PCC}=0} = \frac{1}{s(s^2C_fL_fL_g + L_f + L_g)} \tag{5}$$

Finally, the inverter output admittance can be defined as:

$$Y_C(S) = \frac{i_g}{v_{PCC}}|_{i_g^*=0} = \frac{Y_O}{1 + G_cG_dY_M} = \frac{s^2C_fL_f + 1}{s^3C_fL_fL_g + s(L_f + L_g) + Ke^{-1.5T_Ss}} \tag{6}$$

$$Y_G(j\omega) = \frac{1}{j\omega L_G + R_G}$$

Minor loop gain is given by

$$T_{MA} = \frac{Y_{SA}}{Y_{LA}} \qquad (or) \qquad T_{MA} = \frac{Y_{SG}}{Y_{LA}}$$

2.1. Passivity-Based Stability Analysis of Inverter Output Impedance

2.1.1. Concept of Passivity

DEFINITION: - It is defined the passive network, i.e., impedances Z(s), as a necessary and sufficient condition that a linear networks considering time and energy relation, is passive if its impedance is a positive real function.

$$\text{i.e.} \qquad \text{Re}\int_{-\infty}^{t} v^*(\tau)i(\tau)d\tau \geq 0\,, \quad \text{for all } t > -\infty\,,$$

The total energy delivered to the network becomes [10];

$$\frac{1}{\Pi}\int_{0}^{+\infty} \mathrm{Re}[Z(j\omega)]\left\|I(j\omega)\right\|^2 d\omega > 0,$$

Which impose that $\mathrm{Re}[Z(j\omega)] \geq 0$ at each frequency [11].

This criterion guarantees the phase angle of impedance Z(s) to be in a passive range, given by [−90◦, +90◦]. If we assume that our complex impedance network is composed of many sub-systems, then the stability of the system is determined by its impedance relations. Recalling, if there are only passive sub-systems, the maximum phase angle of the interconnected system must be in the $[-180°, +180°]$ which never encircles (−1, j0) in the Nyquist plot, resulting in a stable system. Therefore, if we put the responsibility on each connected inverter by keeping the common rule of passivity, the entire system can achieve stable operation at all-time [12].

2.1.2. Pole -Zero Frequencies of Inverter Output Admittance

Figure.3&4 shows typical Bode diagrams of grid current controlled inverter with LCL filter and two different possible designs. Both filter designs result in an inverter output admittance, which has notable changes in the magnitude and phase frequency responses. For example, the inverter admittance magnitude has a pronounced dip (anti-resonance) at a frequency ω_d is given by:

$$\omega_d = \sqrt{C_f L_f}^{-1} \quad (7)$$

Which is derived from the double zero's shown in (6).New terms are defined to confine the area of analysis, therefore the LCL filter resonance frequency ω_{res} and the critical frequency of the inverter ω_c is given by:

$$\omega_{res} = \frac{\sqrt{(L_f + L_g)}}{\sqrt{(L_f L_g C_f}} \quad (8)$$

$$\omega_c = \frac{\pi}{3T_s} \quad (9)$$

The critical frequency of the inverter ω_c is one-sixth of the sampling frequency.

$$\text{i.e.} \quad \omega_c = \frac{f_s}{6}$$

If $\omega_{res} > \omega_c$ is satisfied, then the inverter does not need resonance damping for its stand-alone stable operation [13].

Lastly, the Nyquist frequency ω_{NQ} is defined as the half of the sampling frequency.

$$\text{i.e. } \omega_{NQ} = \frac{f_s}{2}$$

Likewise, the locations of the anti-resonance frequency ω_d with respect to ω_c which are $\omega_d > \omega_c$ and $\omega_d < \omega_c$, make two distinctive ways of classifying The non-passive region in Figure. 3&4. The phases of the two admittances exceed the passive range [−90◦, +90◦] in the interval of (ω_d, ω_c) or (ω_d, ω_c), respectively, even though the inverter is designed stable as stand-alone. Due to their inductive dominant nature characteristics, the phase angle of Y_C starts with 0◦ and ends with −90◦ in both cases. Additionally, the phase angle degradations are introduced by the time delay term G_d until they reach ω_d and where the 180◦ phase jump occurs. Therefore, the time delay and the parallel resonance frequency ω_d are the main reason of passivity violation of the inverter.

2.1.3. Non-Passive Range of Inverter Output Admittance

As explained in [12], the passivity violation can be identifies by inspecting the existence of the negative real part of the output admittance:

$$\Re(Y_C(j\omega)) = \frac{K\cos(1.5T_s\omega)(1-\omega^2 C_f L_f)}{(K\sin(1.5T_s\omega)+\omega(\omega^2 C_f L_f L_g - L_f - L_g))^2 + (K\cos(1.5T_s\omega))^2} \quad (10)$$

Eq.(10) identifies a factor which determines the sign of the real part of Y_C [14]. Since the denominator is always greater than 0, the only factor which determines the sign is the cosine function (which comes from the time delay (G_d) and the anti-resonance term ω_d . In Figure. 3&4 the plots of each significant term in the numerator of Eq.(10), shown in above and their combined polarities are shown and both determine the non-passive region of the inverter. The cosine term changes its polarity at ω_c and it changes to positive again at the Nyquist frequency ω_{NQ} .The ($(1-\omega^2 C_f L_f)$ term is drawn for different frequencies of ω_d .There are three different ranges depends on the different values of ω_d .

When $\omega_d < \omega_c$, the non-passive region becomes [ω_d , ω_c],

$\omega_d > \omega_c$, the non-passive region becomes [ω_c , ω_d] and

$\omega_d = \omega_c$, the non-passive region disappears [15] and the system becomes stable for all passive network admittance.

The frequency range for harmonic analysis is limited for easy explanation to the Nyquist sampling frequency ω_{NQ} . However, above the Nyquist frequency, there may be issues, which still need to be investigated [16]. Therefore, this paper analyses the non-passive region of the LCL-filtered grid connected inverter, where the stability may be affected by the passive grid impedances with frequencies up to ω_{NQ} .

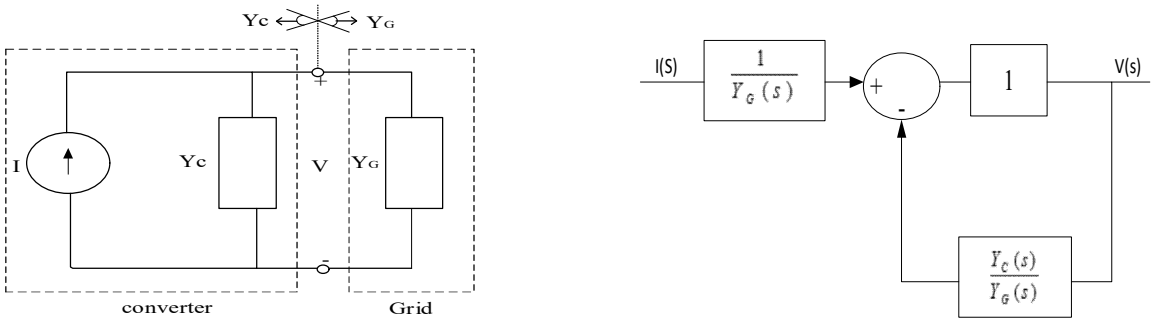

Figure 2. (a) The Small-signal admittance model is connected (or) disconnected to grid with current source; 2. (b) Minor loop gain transfer function framing.

3. Stability Analysis and Results for Different Grid Impedances and the Influence of Inverter Disconnection

In this section, stability regions of the inverter output admittance Y_C with different grid admittance Y_G are described. By using the graphical interpretation with IBSC, the non-passive region of the inverter can provide the possible forbidden regions of the passive grid admittances. Thus the critical grid admittance and the sufficient grid conditions for stable operation of the inverter can be drawn.

3.1. Impedance Based Stability Analysis (IBSC)

The IBSC uses terminal impedance/admittance characteristics of the converter output (Y_C) and grid admittances (Y_G) to find out the interconnected system stability as shown in Figure 2(a). The stability of the interconnected system can be identifies by the so called minor loop gain L_M [4] shown in Figure 2(b) and defined as:

$$L_M = \frac{Y_C}{Y_G} \tag{11}$$

For stability analysis, the magnitude condition $|Y_C| > |Y_G|$ and the negative phase angle crossover condition ($\angle Y_C - \angle Y_G = -\pi \pm 2\pi N$) should be satisfied.

3.1.1 Influence of Pure Inductive Grid Impedance

In order to find the magnitude condition for the pure inductive grid, the admittance magnitude of the non-passive region of the inverter $|Y_C(j\omega)|$ is needed. Since the given grid impedance is passive, the frequency range of concern is limited to the non-passive range of the inverter. The critical frequency ω_c is the reference mark of the non-passive region and where the phase of the inverter crosses its $\pm 90°$.

As a result, the magnitude comparison at ω_c becomes the first step to check the stability of the interconnected system. For the pure inductive grid, the admittance and the critical inductance value of the grid inductance L_G can be calculated by equating the grid admittance Eq.(12) to the output admittance of the inverter Eq.(6) at the critical frequency ω_c as follows:

$$Y_G(j\omega) = \frac{1}{j\omega L_G + R_G} \tag{12}$$

When the grid inductance L_G increases, the admittance line |YG| (solid line) moves downwards as illustrated with dashed line in Figure 3. The area for satisfying the magnitude condition $|Y_C| > |Y_G|$ starts to be broadened. Then, the frequency at negative crossover takes place ($\angle Y_C - \angle Y_G = -\pi \pm 2\pi N$), in this case ω_c, starts to be included in the magnitude inversion region as shown in Figure 3(a). However, depending on the anti-resonance frequency ω_d, the phase difference of the two admittances can be zero, which is the most stable condition, as shown in Figure 3(a)&4(a), 3(b)&4(b) for unstable cases. It is from the phase angle of pure inductive grid admittance ($-90°$).Therefore, the pure inductive grid can make the system unstable only when $\omega_d < \omega_c$ and L_G larger than in Eq.(13) is shown below,

$$L_G = \frac{\sqrt{K^2 \cos^2(1.5T_s\omega_c) + \sin(1.5T_s\omega_c) + \omega_c(\omega_c^2 C_f L_f L_g - L_f - L_g))^2}}{\omega_c \left|1 - \omega^2 C_f L_f\right|} \tag{13}$$

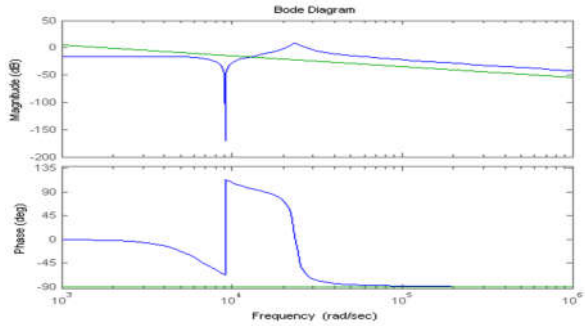

Figure 3a. Stable Case ($\omega_d < \omega_c$).

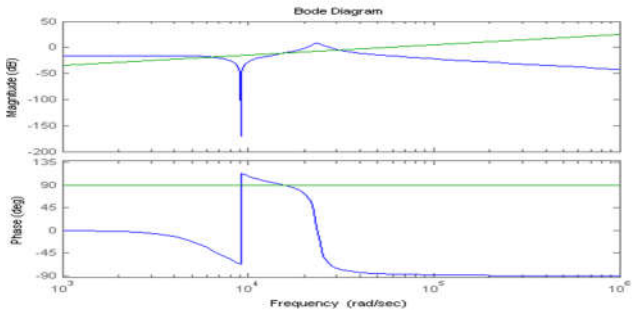

Figure 4a.Stable Case ($\omega_d < \omega_c$).

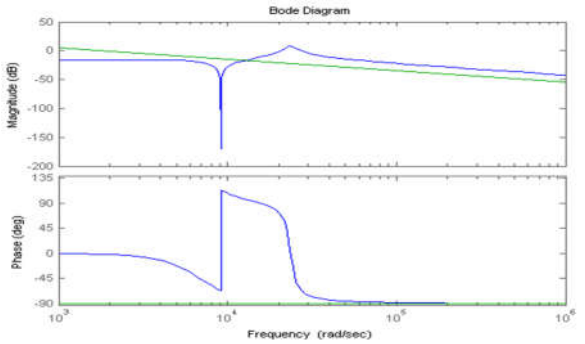

Figure 3b. unstable Case ($\omega_d > \omega_c$).

Figure 3.Stable and unstable region of grid inverter in pure inductive grid.

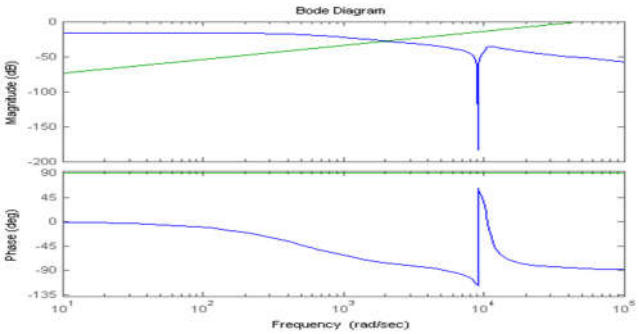

Figure 4b.unstable Case ($\omega_d > \omega_c$).

Figure 4.Stable and unstable region of grid inverter in pure capacitive grid.

3.1.2. Influence of Pure Capacitive Grid Impedance

Similarly, the critical frequency is also analyzed for the capacitive grid which may occur if the inverter is connected with the grid through long underground cables. The stability analysis for variable capacitance C_G works inversely as the L_G in the inductive grid impedance. By the same method as in the pure inductive grid, boundary capacitance value can be found by equating the grid admittance Eq.(14) with the output admittance of the inverter Y_C Eq.(6) at the critical frequency ω_c :

$$Y_G(j\omega) = j\omega C_G \qquad (14)$$

The grid admittance $|Y_G|$ (green solid line) moves downwards as C_G decrease. Different from the pure inductive grid case, the phase angle of Y_G is fixed to $+90°$ in Figure.4. The interconnected system becomes unstable only when $\omega_d > \omega_c$ and C_G is lower than the boundary value in Eq.(15).

$$C_G = \frac{\left|1-\omega^2 C_f L_f\right|}{\omega_c \sqrt{K^2 \cos^2(1.5T_s\omega_c) + (K\sin(1.5T_s\omega_c) + \omega_c(\omega_c{}^2 C_f L_f L_g - L_f - L_g))^2}} \qquad (15)$$

3.1.3. Influence of Resistive- Inductive (RL) Grid Impedance

As it is explained in the previous sections, the inductive and capacitive grid impedance Creates problems for the inverter only with $\omega_d > \omega_c$ as explained in Eq.(13). Furthermore, if the grid impedance contains resistive impedance, the system becomes relatively more stable by its resistive damping as shown by:

$$Y_G(j\omega) = \frac{1}{j\omega L_G + R_G} \tag{16}$$

However, a complexity problem appears on managing the equation when the grid impedance contains a resistive value. Rules for judging the unstable region become more complicated and an explicit solution for satisfying the equation is more difficult to be obtained. Therefore, another conservative way of defining the system stability region is necessary to get an analytical solution.

$$\frac{1}{\sqrt{L_G^2\omega_c^2 + R_G^2}} \geq \frac{\left|1-\omega^2 C_f L_f\right|}{\sqrt{K^2\cos^2(1.5T_s\omega_c) + (K\sin(1.5T_s\omega_c) + \omega_c(\omega_c^2 C_f L_f L_g - L_f - L_g))^2}} \tag{17}$$

If the magnitude condition $|Y_G(j\omega)| \geq |Y_C(j\omega)|$ is satisfied in the interval $\omega_d < \omega < \omega_c$, then the inverter is always stable. Therefore, the sufficient magnitude condition is derived in Eq.(17), and is illustrated in the magnitude plot in Figure 5.If the magnitude condition is not satisfied, it does not mean that the system is unstable. The system can be stable with large R_G, which can be explained by its resistive damping. Therefore, the additional phase condition has to be applied in order not to create a too conservative condition.

A maximum non-passive phase angle, which creates the worst condition of the phase angle difference, is used to define the sufficient conditions in the phase plot illustrated in Figure 5. The terms α, β are as follows with respect to Eq.(18) & Eq.(19),

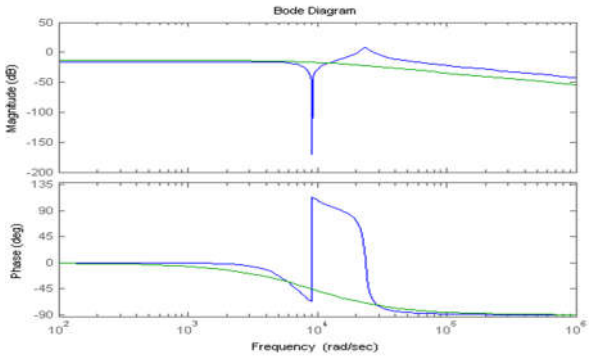

Figure5. Sufficient stable condition for grid Inverter with RL grid impedance for ωd <ω c.

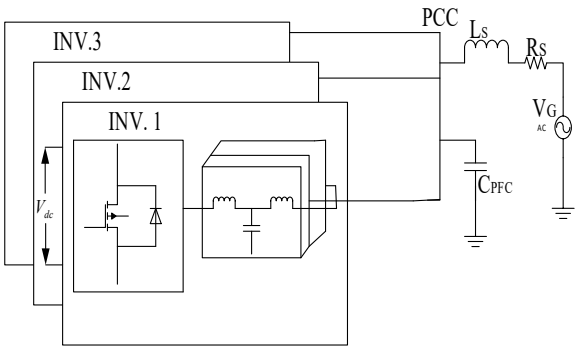

Figure 6. Single line diagram of Three paralleled Inverters connected to grid

$$\alpha(\omega) = \tan^{-1}(\tan(1.5T_s\omega) + \frac{\omega(\omega^2 C_f L_f L_g - (L_f + L_g))}{K\cos(1.5T_s\omega)}) \pm \frac{\pi}{2} \Big|_{\substack{+\omega_r < \omega_c \\ -\omega_r > \omega_c}} \tag{18}$$

$$\beta(\omega) = \tan^{-1}(-\frac{L_G}{R_G}\omega) + \frac{\pi}{2} \tag{19}$$

The abrupt phase change appears at the frequency ω_d and it becomes the maximum phase shift angle. Eq. (20) shows the condition in which the phase angle of the inverter degrades faster than the phase drop of the grid impedance in the non-passive region. It means that the worst phase condition can be found only by checking the

phase difference at ω_d. If both Eq. (20) and Eq. (21) are satisfied, then the inverter with RL grid impedance is always stable.

$$\frac{9T_s^{\,2}(L_f + L_g) - \pi^2 L_f L_g C_f}{(3T_s^{\,3})K} > 1 \tag{20}$$

$$\alpha(\omega_d) \le \beta(\omega_d) \tag{21}$$

3.2. Stability Analysis of Multi-Paralleled Inverter Connected to Grid

In power distribution system there are many connected DG units, some of them can be non-passive inherently and they may affect the system stability as well. In this case, the grid impedance seen from one grid inverter cannot be considered as purely passive impedances but is affected by other inverters or non-passive active loads; therefore, they create non-passive grid impedance which is even more difficult to be estimated. Therefore, a parameter sweep method and random case simulations are adopted to check the distribution system stability. Figure 6. Three paralleled inverters connected to grid is considered for assessment of harmonic stability and Capacitor bank is connected at PCC to improve the Power factor. These inverters are designed with respect to passively damped LCL-filter with their power ratings as per the Cigré LV benchmark system [17]. Here two types of case studies are conducted, first one is the grid impedance variation and the second one is changes in number of paralleled inverters are connected to grid. All cases harmonic stability is analysied by the IBSC with help of root locus plot, It is verified in the MATLAB simulation. Single line diagram of the grid tied inverter with control system for simulation implementation as shown in figure 7.

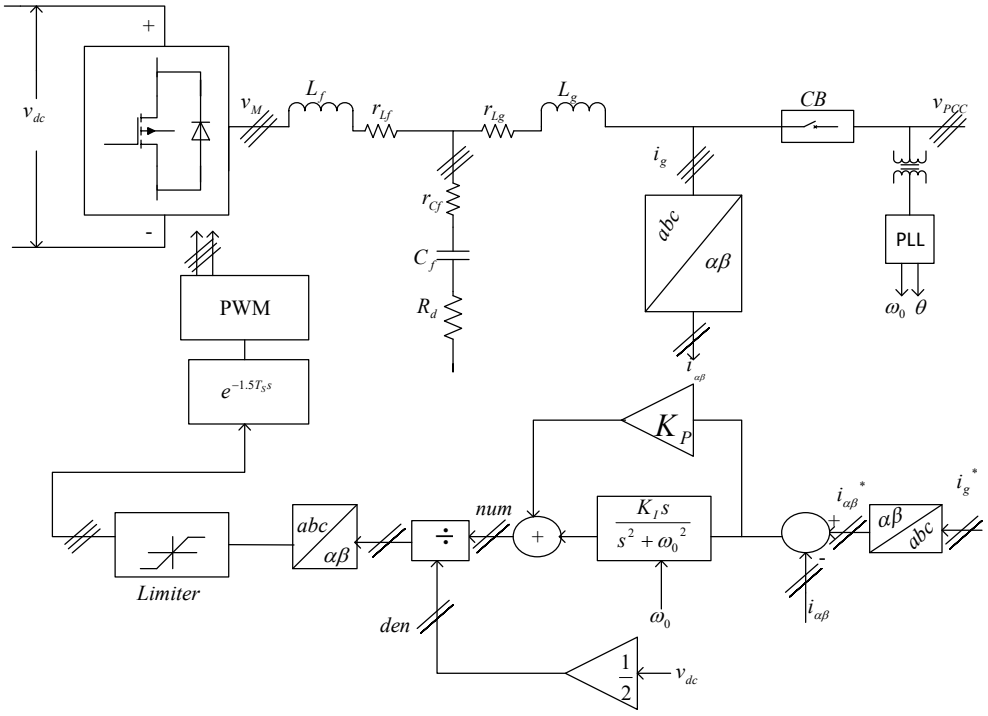

Figure7. The inverter tied to grid with control diagram for MATLAB-Simulink implementation.

Table.1. Specification and Parameters of the grid inverters

Inverter Name		INV.1	INV.2	INV.3
Power Rating[KVA]		5.6	3.5	10.5
Switching Frequency[Hz]		10		15
DC Link Voltage			600V	
Filter Values	L_g [mH]	20	22	24
	r_{Lf} [mH]	22/0.2	15/0.4	2/7
	r_{Cf} [mf]	0.22	0.3	1.7
Parasitic Values	r_{Lg} [mΩ]	11.4	15.7	66.8
	L_g [mH]	7.5	11	21.5
	r_{Lf} [mH]	2.9	3.9	22.3
Control Gain	K_p	8.05	28.8	16.6
	K_I	1000	1500	1500

3.2.1. Case Studies of Varying Grid Impedance

Three paralleled inverters tied to the grid has grid impedance (Z_s) , power factor correction capacitor (PFC) is connected at PCC to improve power factor of the system. The Grid admittance (Y_{SG}) and the load admittance (Y_{LG}) are given in Esq.(22) & (23).

$$Y_{SG} = \frac{1}{R_S + sL_S} \tag{22}$$

Where R_S - Grid resistance, L_S - Grid inductance as shown in Figure.6

$$Y_{LG} = Y_{CPFC} + \sum_{X=1}^{3} Y_{CLX}$$

$$Y_{LG} = SC_{PFC} + Y_{CL1} + Y_{CL2} + Y_{CL3} \tag{23}$$

Where Y_{CPFC} denotes the admittance of capacitor $CPFC$ as shown in Figure. 6. Finally, the minor loop gain T_{MG} is obtained as follows:

$$T_{MG} = \frac{Y_{SG}}{Y_{LG}} \tag{24}$$

If the variation in load admittance Y_{LG} results effects the minor loop gains (T_{MG}), the root locus plots are plotted for the system with the fixed grid resistance and by varying the grid inductance, ranging from L_S value155uH to 400uH, the poles of the system lies on the left side of the S-plane which represents the system is stable and when grid inductance increases the Total Harmonic distortion of the grid current reduces.

Case 1: Grid impedance $Z_s = 0.1 + j\omega 155uH$

In this case the all three inverters are connected to grid and the grid inductance is taken as 155uH, here the inverters injecting the currents are INV1=10A, INV2=8A, INV3=5A to the grid and the simulation results of Root locus plot, grid voltage, grid current and THD of grid current are shown in Figures 8,9,10&11.

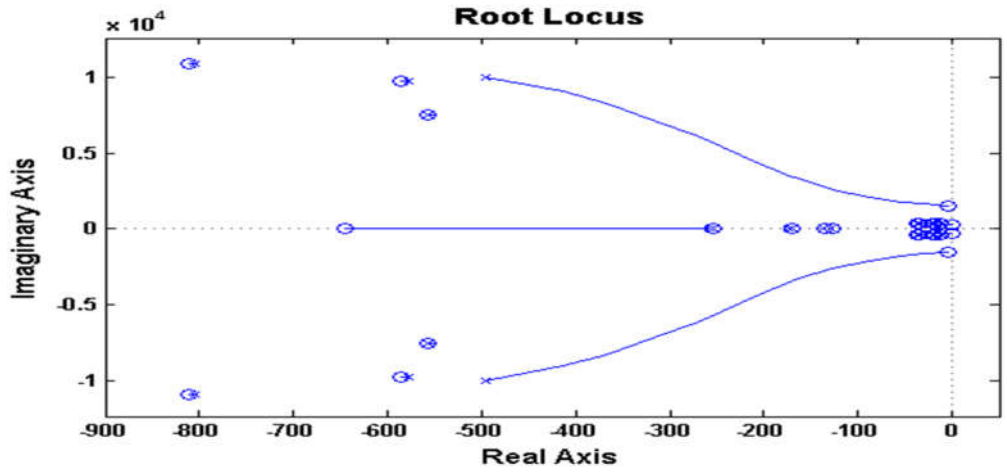

Figure 8. Root locus Plot of the System

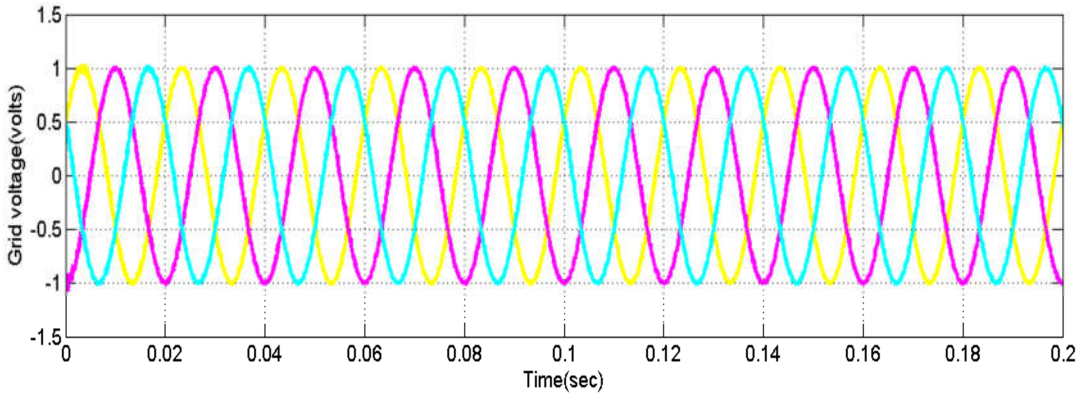

Figure 9. Grid voltage(V)

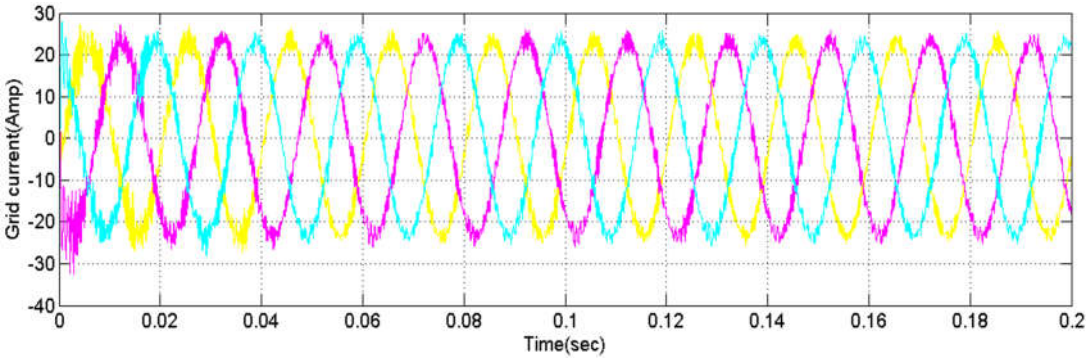

Figure 10. Grid current(A)

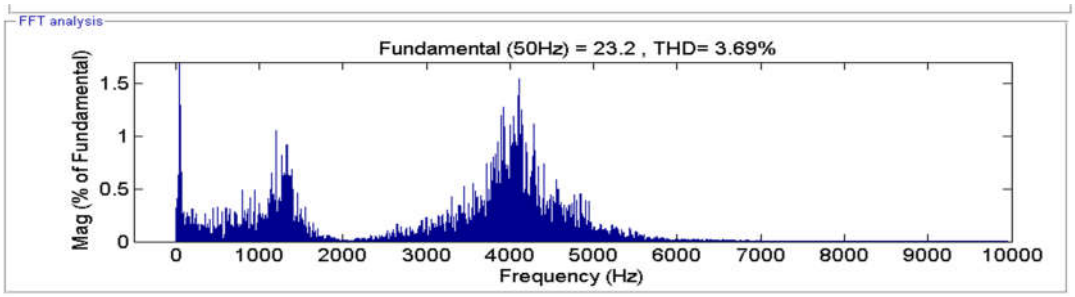

Figure 11. THD of the grid Current(%)

Case 2: **Grid impedance** $Z_s = 0.1 + j\omega 400uH$

In this case the all three inverters are connected to grid and the grid inductance is 400uH, here the inverters injecting the currents are INV1=10A, INV2=8A, INV3=5A to the grid and the simulation results of Root locus, grid voltage, grid current and THD of grid current are shown in Figures,12, 9,13 &14.

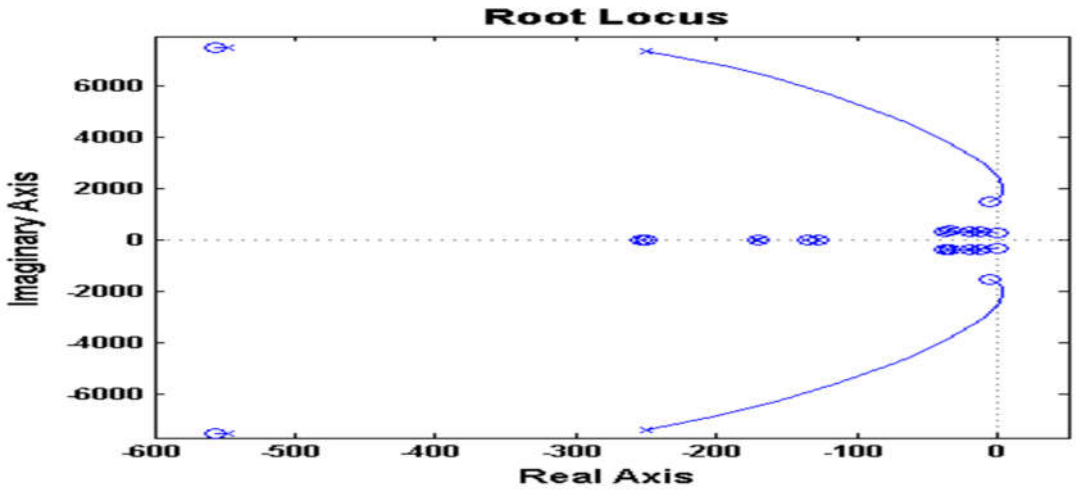

Figure 12. Root locus plot of the System

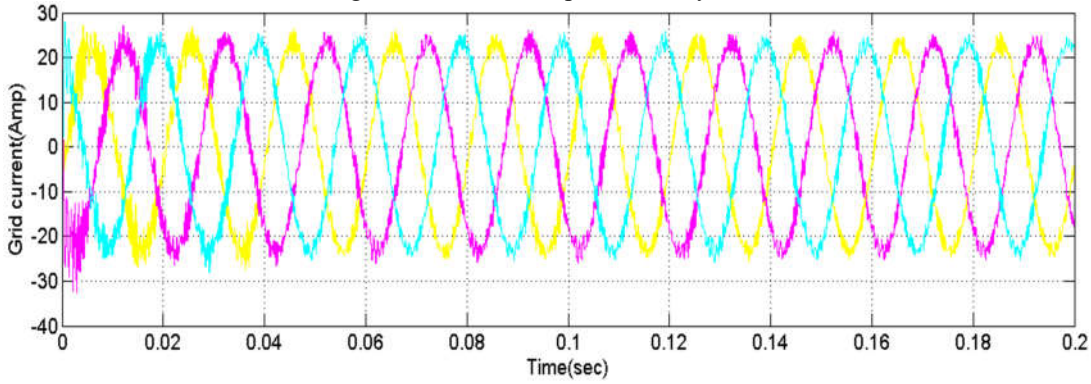

Figure 13. Grid Current(A)

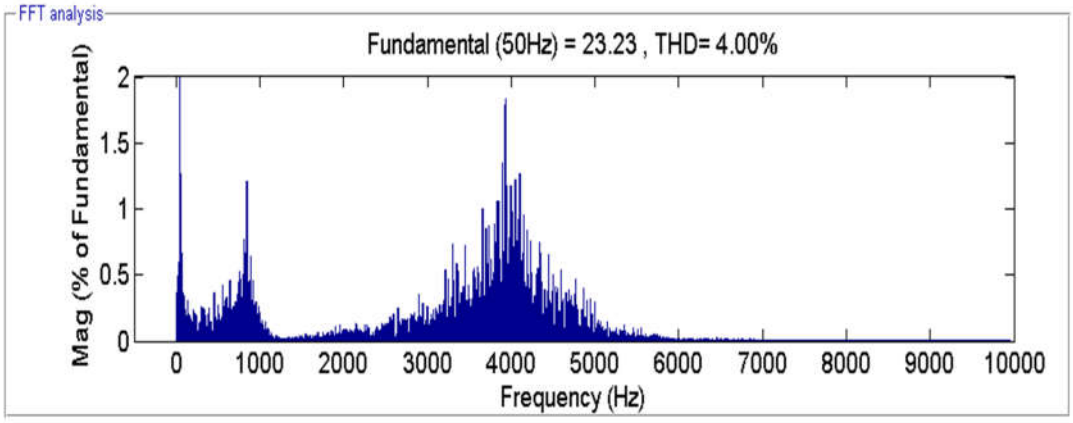

Figure 14. THD of grid Current Graph (%)

3.2.2. Case Studies of Inverter Disconnection from the Grid

Case1: $Y_{LG} = SC_{PFC} + Y_{CL1} + Y_{CL3}$

In this case the two inverters are connected to grid and the grid inductance is maintained at 400uH, here the inverters injecting the currents are INV1=10A, INV2=OFF, INV3=5A to the grid and the simulation results of Root locus of the system ,grid voltage, grid current and THD of the grid current are shown in Figures 15,9,16&17.

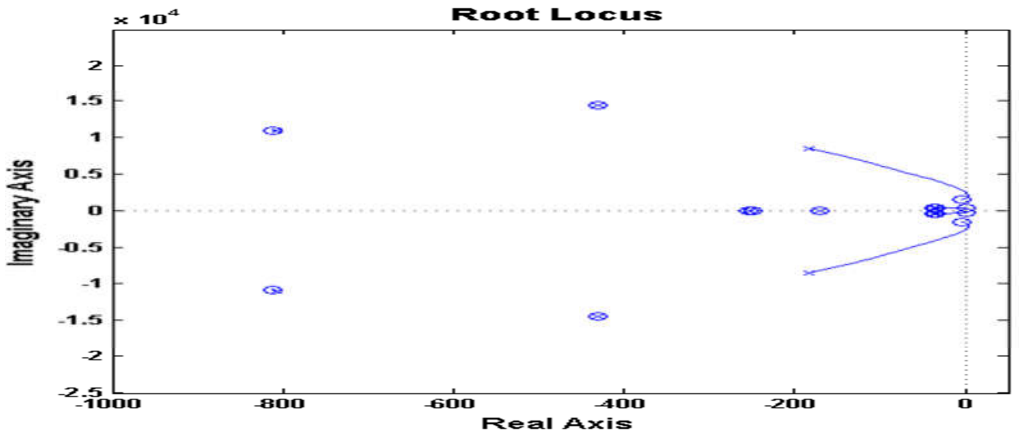

Figure15. Root locus Plot of the System

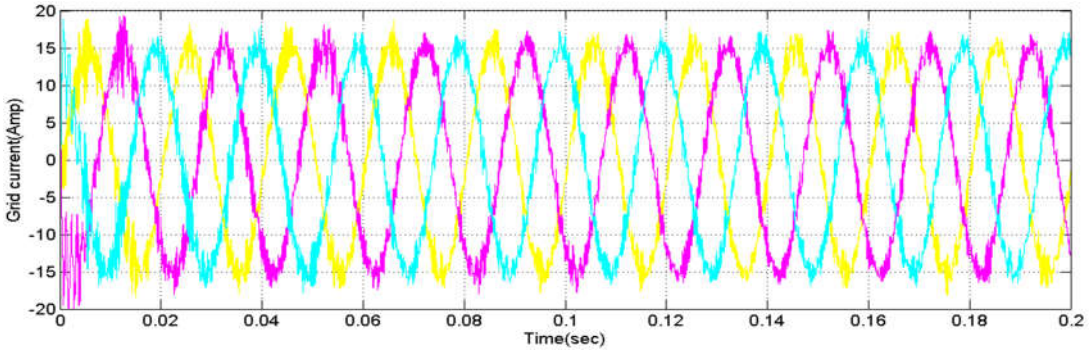

Figure 16. Grid current at INV1 and INV3 are Connected to Grid(A).

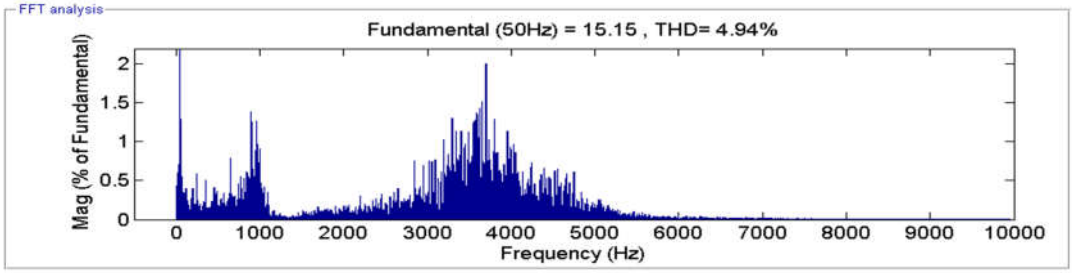

Figure17. THD of Grid Current (%)

Case2: $Y_{LG} = SC_{PFC} + Y_{CL2} + Y_{CL3}$

In this case Two inverters are connected to grid and the grid inductance same, here the inverters injecting the currents are INV1=OFF, INV2=8A, INV3=5A to the grid and the simulation results of root locus plot, grid voltage, grid current and THD of the grid current are shown in Figures 18,9,19 & 20.

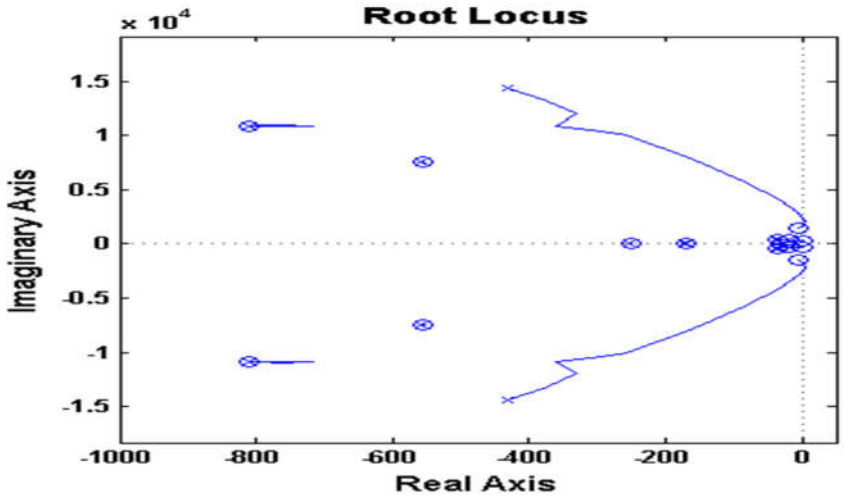

Figure 18. Root locus Plot of the System

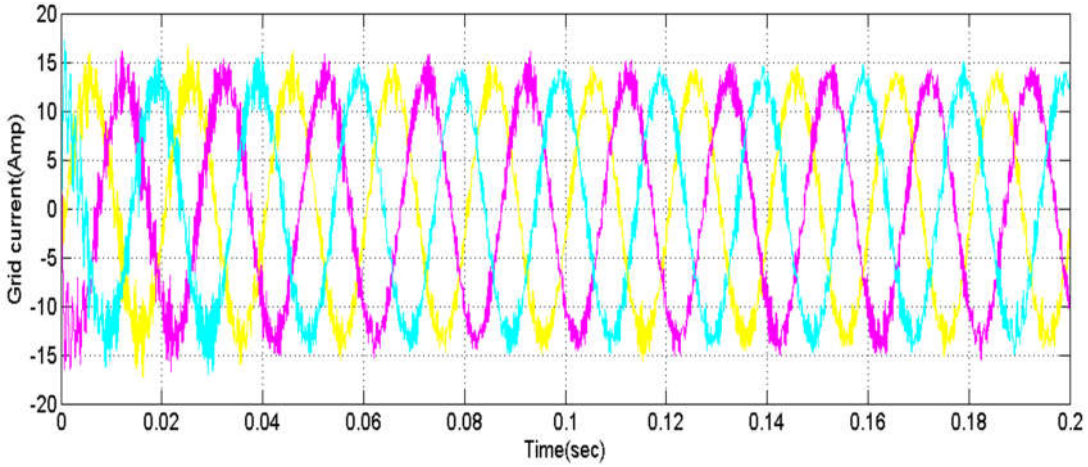

Figure 19. Grid current (A)

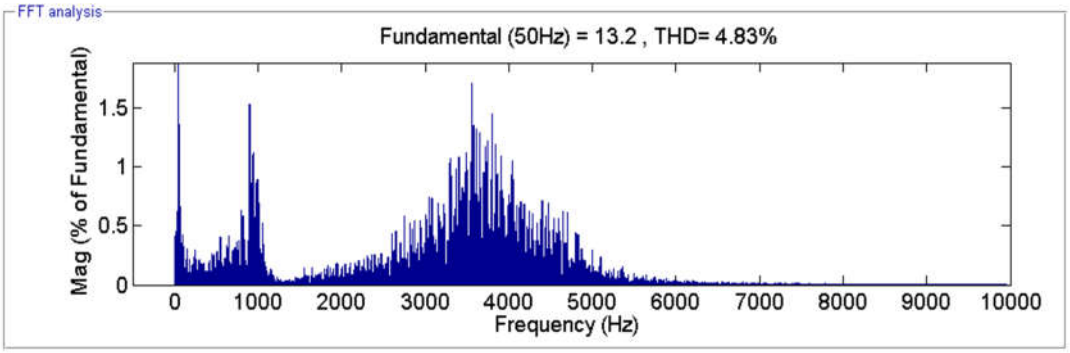

Figure 20. THD of Grid Current(%)

4. Conclusion

In this work the reasones for instability between the grid connected inverter and passive grid impedance is first explained by using the passive based approch.With help of the bode plots and necessary condationes are derive to become system is stable with different grid impedances when parallel inverters are connected the grid.analysis of the system become more complex be consedering the all cases.Here 2 cases with different operating condationes are considered to see whether the system stable or not.which showes the hormonic Stability occurs in any case from the above results,moreever quality of the grid current also with in the limit and it is universaly accepted,It is verified in MATLAB simulation.

REFERENCES

[1] X.Wang,F.Blaabjerg,and W.Wu,"Modeling and analysis of harmonic stability in an Ac power- electronics-based power system," IEEE Trans.Power Electron.,vol.8993,no.12,pp.1–1,Dec.2014.

[2] X.Wang,F.Blaabjerg,M.Liserre,Z.Chen,J.He,and Y.Li,"An active damper for stabilizing power-electronics-based AC systems,"IEEETrans.Power Electron.,vol.29,no.7,pp.3318–3329,Jul.2014.

[3] J.H.R.Enslin and P.J.M.Heskes,"Harmonic interaction between a large number of distributed power inverters and the distribution network,"IEEE Trans. Power Electron.,vol.19,no.6,pp.1586–1593,Nov.2004.

[4] "IEEE Recommended Practice and Requirements for Harmonic Control in Electric Power Systems,"IEEE Std 519-2014 (Revision of IEEE Std 519-1992).IEEE Standards Association, NewYork,NY,USA,pp.1–29,2014.

[5] R.D.Middlebrook,"Input filter considerations in design and application of switching regulators,"in Proc.IEEE IAS Annu.Meeting,pp.366–382,1976.

[6] X.Feng,J.Liu,and F.C.Lee,"Impedance specifications for stable DC distributed power systems,"IEEE Trans.Power Electron.,vol.17,no.2,pp.157–162,Mar.2002.

[7] J.Wyatt,L.Chua, J.Gannett,I.Goknar,and D.Green,"Energy concepts in the state-space theory of nonlinear n-ports:PartI-passivity,"IEEETrans.Circuits Syst.,vol.28,no.1,pp.48–61,Jan.1981.

[8] V.Blasko and V.Kaura,"A new mathematical model and control of a three-phase AC-DC voltage source converter,"IEEETrans.Power Electron.,vol.12,no.1,pp.116–123,Jan.1997.

[9] C.Bajracharya,M.Molinas,J.A.Suul and T.M.Undeland," Understanding of tuning techniques of converter controllers for VSC HVDC, "inProc. NordicWorkshop PowerInd .Electron. (NORPIE / 2008),2008,p.8.

[10] D.Youla,L.Castriota,and H.Carlin,"Bounded real scattering matrices and the foundations of linear passive network theory,"IRETrans.Circuit Theory,vol.6,no.1,pp.102–124,Mar.1959.

[11] A.Riccobono and E.Santi,"A novel passivity-based stability criterion (PBSC) for switching converter DC distribution systems,"in Proc.IEEE 27th Appl.Power Electron.Conf.Expo.,pp .2560–2567,Feb.2012.

[12] X.Wang,F.Blaabjerg,and P.C.Loh,"Proportional derivative based stabilizing control of paralleled grid converters with cables in renwable power plants,"in Proc.IEEE Energy Convers.Congress Expo.(ECCE'14),2014,pp.4917–4924.

[13] S.G.Parker,B.P.McGrath,and D.G.Holmes,"Regions of active damping control for LCL filters,"IEEETrans.Ind.Appl.,vol.50,no.1,pp.424–432,Jan.2014.

[14] H.Bai,X.Wang,P.C.Lohand F.Blaabjerg,"Passivity enhancement of grid-tied converter by series LC-filtered active damper,"in Proc.IEEE 7th Energy Convers.Congress Expo.(ECCE'15),2015.

[15]M.Huang,X.Wang,P.C.Loh,and F.Blaabjerg,"LLCL-filtered grid converter with improved stability and robustness,"IEEETrans.Power Electron.,vol.31,no.5,pp.3958–3967,May2016.

[16] Y.Tang,W.Yao,P.Loh and F.Blaabjerg,"Design of LCL-filters with LCL resonance frequencies beyond the Nyquist frequency for grid connected converters,"IEEE J.Emerg .Sel. Topics Power Electron.,vol.4,no.1,pp.3–14, Mar.2015.

[17] Cigre Committee SCC6."Benchmark systems for network integration of renewable and distributed energy resources,"Task Force C6.04.02,Technical Brochure 575,2014.

[18] G.Raisbeck,"A definition of passive linear networks interms of time and energy," J. Appl. Phys., vol.25,no.12,p.1510,May1954.